LANGMUIR Article
Cite This: Langmuir 2018, 34, 1473−1480
pubs.acs.org/Langmuir

Adsorption of Catalytic Nanoparticles onto Polymer Substrates for Controlled Deposition of Microcapsule Metal Shells

James P. Hitchcock,*[,‡] Alison L. Tasker,[†] Kirsty Stark,[†] Andrew Leeson,[†] Elaine A. Baxter,[§] Simon Biggs,[†] and Olivier J. Cayre[†]

[‡]School of Chemical and Process Engineering, University of Leeds, Woodhouse Lane, Leeds, LS2 9JT, United Kingdom
[†]School of Chemical Engineering, University of Queensland, St. Lucia, Queensland 4072, Australia
[§]HFC Prestige Services (U.K.) Ltd, Prune Hill, Rusham Park, Egham TW20 9NA, United Kingdom

Supporting Information

ABSTRACT: Efficient encapsulation of small chemical molecules and their controlled targeted delivery provides a very important challenge to be overcome for a wide range of industrial applications. Typically rapid diffusion of these actives across capsule walls has so far prevented the development of a versatile widely applicable solution. In an earlier publication, we have shown that thin metal shells are able to permanently retain small molecules. The critical step in the microcapsule synthesis is the formation of a strongly adsorbed, dense monolayer of catalytic nanoparticles on the surface as this affects the secondary metal film quality. Control over Pt-nanoparticle adsorption density and a clear understanding of Pt-nanoparticle adsorption kinetics is therefore paramount. Maximising the density of heterogeneous catalysts on surfaces is generally of interest to a broad range of applications. In this work, transmission electron microscopy (TEM) and quartz crystal microbalance (QCM) are used to demonstrate that the concentration of nanoparticle polymer stabilizer used during particle synthesis and nanoparticle suspension concentration can be used to control nanoparticle surface adsorption density. We demonstrate that excess polymer, which is often used in nanoparticle synthesis but rarely discussed as an important parameter in the literature, can compete with and thus drastically affect the adsorption of the Pt-nanoparticles.

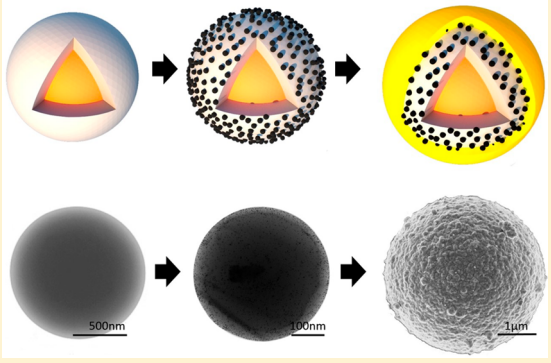

INTRODUCTION

Efficient encapsulation of chemicals and their controlled targeted delivery is an area of significant academic and industrial interest. Despite recent advances, significant challenges remain for the encapsulation of low molecular weight molecules, as typical polymer microcapsule shells cannot prevent leaching of such core materials. In a previous research article,[1] we developed a method for the efficient encapsulation of small volatile molecules using impermeable metal shells

The most critical step in this procedure is the formation of a strongly adsorbed and dense monolayer of catalytic nanoparticles at the interface to be coated with metal. Indeed, the 2D surface density and the homogeneity of the adsorbed nanoparticles are the key variables that affect the quality of the subsequently deposited continuous metal films. A good understanding of the nanoparticle adsorption kinetics and energetics and their influence over the adsorption is therefore paramount if we are to achieve reliable permanent encapsulation of the active molecules in the core. In addition, the preferred electroless deposition catalysts are usually expensive noble metals, it is important therefore that they are used efficiently in capsule manufacturing. This article investigates the various parameters that can influence the adsorption process so that the final adsorbed nanoparticle density can be controlled efficiently.

Combining polymers and nanoparticles to design functional microparticles has been used extensively in the literature.,[2−13] for example to synthesize microcapsules with light responsive release capabilities using optically addressable nanoparticles.[3,4,9,11] Most applications however describe the use of polymer particles or polymer-coated particles as substrates to support catalytic nanoparticles. These hybrid particles serve to improve the recoverability and stability of nanoparticle catalysts, while retaining most of their high surface area.[2,5−8] In particular, several articles describe the physical adsorption of nanoparticles onto preformed polymeric particle interfaces. In these cases, control over nanoparticle surface density is paramount, highlighting the importance of understanding the adsorption process, which this work aims to achieve for our particular system.

Received: August 15, 2017
Revised: December 5, 2017
Published: December 11, 2017

DOI: 10.1021/acs.langmuir.7b02874
Langmuir 2018, 34, 1473−1480

In an aqueous environment, nanoparticles can be located at the surface of a polymeric particle either by reducing preadsorbed metal ions at the polymer−solution interface, or by using preprepared charged or highly polar nanoparticles to physically adsorb onto the surface.[7,10,11,14] Alternatively, nanoparticles can be made to adsorb at a polymer particle interface by altering the dispersions stability or charge using electrolyte concentration or pH.[5] A further method was also exemplified by De Geest et al.,[11] who alternately adsorbed a positive polyelectrolyte and negatively charged gold nanoparticles onto emulsion drop interfaces to build multilayered capsules. Similarly, Antipov et al.[7] used layer by layer alternate deposition of oppositely charged polymers to create a film which itself acted as the reducing agent for silver ions in the bulk, resulting in silver nanoparticle coated particles.

In this work, which attempts to optimize the nanoparticle adsorption process onto polymer microcapsules, platinum nanoparticles stabilized with poly(vinylpyrrolidone) (PVP) are physically adsorbed on the poly(ethyl methacrylate) (pEMA) shell surface of microcapsules. Platinum is a very efficient catalyst for gold growth, via electroless deposition and is therefore an ideal system with respect to the eventual deposition of a continuous metal film onto polymer microcapsules.[15] In addition, the polar nature of PVP allows it to physisorb onto a broad range of interfaces.[16] PVP is also highly solvated in pure water and therefore, as a particle stabilizer, it provides steric hindrance between platinum nanoparticles dispersed in an aqueous phase. These qualities allow for the production of stable Pt-nanoparticle dispersions with a strong affinity to a broad range of surfaces which are able to direct the reduction of gold salts due to their good catalytic activity.

This work uses transmission electron microscopy (TEM) and quartz crystal microbalance (QCM) to explore Pt-nanoparticle adsorption onto 2-D pEMA substrates, which are used as a model analogue surface for polymer microcapsules. The effect of PVP stabilizer concentration on Pt-nanoparticle synthesis and their subsequent ability to adsorb on a pEMA interface is explored initially. From this study, an optimized nanoparticle suspension was chosen for adsorption studies on the 2-D model pEMA films. Subsequently, nanoparticle adsorption kinetics and their influence on the final density of adsorbed nanoparticles were explored in detail. The data gathered in this part of the work then guided the conditions chosen for exploring the adsorption of nanoparticles onto the (3-D) capsule surfaces.

EXPERIMENTAL SECTION

Materials. Poly(ethyl methacrylate) (pEMA) (120 kDa), cetyltrimethylammonium bromide (CTAB) 98%, toluene 99%, dichloromethane (DCM) > 99%, poly(vinylpyrrolidone) (PVP) (40 kDa), chloroplatinic acid (H_2PtCl_6) 99%, chloroauric acid ($HAuCl_4$) 99.99%, 35 vol % hydrogen peroxide solution in water, and sodium borohydride ($NaBH_4$) 99% were all obtained from Sigma-Aldrich and used as received. All solutions were prepared using ultrapure Milli-Q water (resistivity ∼ 18 MΩ·cm^{-1}).

Synthesis of Polymeric Capsules with Oil Core via Cosolvent Extraction. pEMA (10 g) was dissolved in DCM (81 g), and toluene (14 g) was added and mixed to form a single phase. This was used as the emulsion dispersed phase. CTAB (0.28 g) was dissolved in Milli-Q water to form the continuous phase. Then 7 mL of each phase was emulsified together at 15 000 rpm for 2 min using an IKA T25 Ultra-Turrax instrument. The emulsion was then stirred magnetically at 400 rpm while a further 86 mL of continuous phase was poured in slowly. The diluted emulsion was then stirred at 400 rpm for 24 h at room temperature to allow full extraction of the DCM. The resulting capsules underwent three washing steps via centrifugation at 1000*g* for 5 min, following which the supernatant was removed and replaced with fresh Milli-Q water. Finally, the capsules were redispersed in 50 mL of Milli-Q water.

Platinum Nanoparticle Synthesis. Pt-nanoparticle synthesis was adapted from the synthesis described in our previous work.[1] In this procedure, $H_2PtCl_6{\cdot}6H_2O$ (0.23 g) was first added to a PVP solution and stirred to dissolve (Pt-nanoparticles were synthesized using a range of concentrations of PVP from 2.0 to 0.0015 wt %). Then 3 mL of $NaBH_4$ (0.5 M (0.189g in 10 mL)) was subsequently added to the prepared solution with vigorous stirring for 2 min upon which the solution turned dark which is an indication of metal precipitation. Resulting suspensions were characterized through TEM confirming the formation of Pt nanoparticles. Equation 1 describes the chemical equation for this particular process.

$$NaBH_4 + H_2PtCl_6 + 3H_2O \rightarrow Pt(s) + H_3BO_3 + 5HCl + NaCl + 2H_2(g) \quad (1)$$

Spin- and Dip-Coating of QCM Crystals and TEM Grids. A WS-400B-6NP/LITE spin-coater (200 rpm for 2 min) was used to deposit thin films of polymer onto the QCM crystals. Surfaces to be spin-coated were cleaned with a detergent solution, rinsed thoroughly with Milli-Q water, dried with compressed air, and then washed in 100% ethanol and dried again with compressed air. Then 1 mL of the coating solution (1g·L^{-1} pEMA in DCM) was deposited via glass pipet directly onto the surface to be coated. A Veeco BioScope atomic force microscope (AFM) was used to assess the resulting pEMA films for thickness. In order to coat TEM grids with pEMA, grids were dipped into the same solution of pEMA in DCM (0.1 wt % in DCM (1g·L^{-1})) for ∼1 s and were then blotted onto a tissue to remove excess pEMA solution and allowed to dry for 1 h.

Adsorption of PVP Stabilized Pt Nanoparticles at Polymeric Interfaces. For 2-D adsorption studies, adsorption of Pt-nanoparticles onto pEMA dip-coated TEM grids was achieved by placing the grids into a suspension of Pt-nanoparticles, diluted to known concentrations with Milli-Q water, for known time periods. TEM grids were then thoroughly washed twice with pure Milli-Q water.

In the case of adsorption studies conducted on the polymeric microcapsules, 2 mL of the microcapsule dispersion (described above) was used. Then 5 mL of the Pt-nanoparticle suspension (described above) was added to the capsule dispersion and mixed for 10 min on a carousel at 30 rpm (the concentration of Pt-nanoparticles was varied in the suspension by dilution, while the volume added to the microcapsule dispersion was kept constant). Following this step, the capsules were immediately washed by centrifugation at 1000*g* for 5 min and the supernatant was replaced with pure Milli-Q water. This operation was repeated three times. The capsules were subsequently redispersed in 30 mL of Milli-Q water.

Microscopy Characterization. The morphology of the microcapsules was studied using an Olympus BX51 optical microscope, a LEO 1530 Gemini field emission gun scanning electron microscope (FEGSEM), and a FEI Tecnai TF20 field emission transmission gun electron microscope (FEGTEM) fitted with a HAADF detector and Gatan Orius SC600A CCD camera. Prior to TEM analysis, samples were dispersed on a TEM grid (holey carbon film, 400 Cu Mesh from Agar Scientific).

Quartz Crystal Microbalance. Experiments were performed using a Q-Sense D300 apparatus. The QCM was used to assess the adsorption of polymers and nanoparticles onto spin coated polymeric films. Before each run, QCM crystals were washed with a detergent solution and rinsed thoroughly with Milli-Q water, piping was renewed and the system was rinsed with warm detergent solution and then Milli-Q water and then was allowed to settle for 20 min prior to the injection of the suspension/solution to be tested. QCM adsorption studies designed to compare Pt-nanoparticle adsorption densities with on washed TEM grids were subjected to a Milli-Q wash cycle. Where necessary, details of concentrations and times of operation are described within the results section. All values were measured for the third overtone of the crystals fundamental frequency

DOI: 10.1021/acs.langmuir.7b02874
Langmuir 2018, 34, 1473−1480

near 15 MHz at room temperature (20 °C). Frequency changes were correlated to the mass change using Sauerbrey's equation.[17]

Pt-Nanoparticles Adsorption Density, Size, and Concentration. Image-J automated image analysis software was used to analyze model 2D nanoparticle adsorption densities and Pt-nanoparticle sizes. TEM images were first adjusted for contrast, the threshold size was then set to a surface area 2−28 nm^2, and the circularity was set to 0.2−1.00. The resulting image was then made binary and the particles were automatically analyzed to record both the average apparent cross sectional area of each nanoparticle and the number per unit area. These surface areas were then used as an approximation of the Pt-nanoparticle cross sectional surface area, assuming nanoparticles were spherical. This surface area was then used to calculate equivalent particle diameters and a size distribution for the suspension. In order to calculate Pt-nanoparticle concentrations, an assumption was made that 100% of the platinum in the platinum salt is converted to Pt-nanoparticles. The size distribution and mass of Pt present was then used to calculate Pt-nanoparticle concentration (4.6×10^{15} mL^{-1}).

TEM was also used to measure Pt-nanoparticle adsorption densities on microcapsule 3D interfaces. Only capsules smaller than ∼500 nm diameter were sufficiently transparent to generate enough contrast between the Pt-nanoparticles and the capsule, in addition the variation in transmitted light intensity across the surface of the spherical polymeric capsule and the fact that both top and bottom surfaces of the capsule were visible meant that automated counting software such as image-J proved not useful. Instead capsules were analyzed manually and apparent nanoparticle surface densities were corrected for capsule curvature and transparency (see the Supporting Information). A NanoSeries Zetasiser (Malvern Nano-ZS) fitted with a He−Ne laser source (633 nm wavelength, 4 mW power) was also used to measure nanoparticle size distributions in suspension.

Polymeric Capsule Size Distribution, Concentration, and Surface Area Calculations. A Malvern hydro 2000SM Mastersizer was used in conjunction with a Malvern "Small Volume Sample Dispersion Unit" to measure size distributions of microcapsules via low angle laser light scattering (LALLS). An average capsule diameter of 2.1 μm $D(0.50)$ and a corresponding total sample surface area of ∼2.03 m^2 were measured and calculated, respectively (see the Supporting Information for calculation). Total final capsule volume post solvent extraction was calculated and used in conjunction with the capsule size distribution to calculate the capsule concentration.

RESULTS AND DISCUSSION

Nanoparticle Synthesis Optimization for Adsorption Studies. This part of the work focused on developing a nanoparticle synthesis protocol to control both the concentration of stabilizing polymer and the nanoparticle diameter. A reproducible synthesis of Pt-nanoparticles was required to ensure comparability of data for adsorption measurements onto the different polymer surfaces of interest. Here, Pt-nanoparticles were synthesized using different concentrations of PVP in the precursor platinum salt solution (chloroplatinic acid), to which a reducing agent (sodium borohydride) is added initiating the reaction. A range of PVP concentrations (0.0015−2 wt %) were used to probe the stability of the resulting nanoparticle suspensions. Pt-nanoparticle, mean core diameter was measured from TEM images using Image-J. Figure 1 shows the evolution of the Pt-nanoparticle core diameter as a function of PVP concentration used in the synthesis (the polymer stabilizer thickness was not determined, as poor density contrast does not allow its resolution by TEM). A small decrease of the Pt-nanoparticle mean core diameter with increasing PVP concentration is seen here; this relationship is expected and has been reported previously in the literature.[18] The Pt-nanoparticle dispersions prepared here remained stable for 6 weeks when stored at 5 °C for PVP concentrations as low as 0.0015 wt %. However, at lower stabilizer concentrations, the dispersions appeared unstable as Pt was observed to precipitate out of the dispersions within only a few hours.

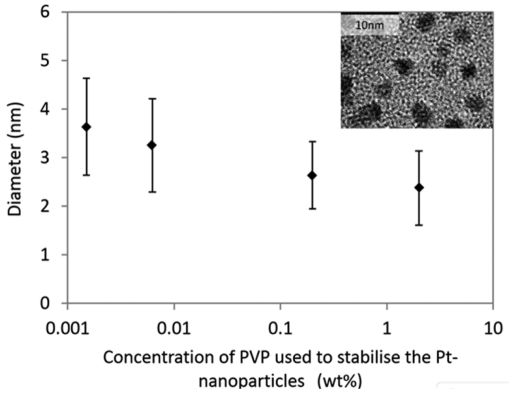

Figure 1. Pt-nanoparticles mean (metal) core diameter as a function of PVP concentration used in the particle synthesis. Data are obtained from image processing (via ImageJ software) transmission electron micrographs obtained for each sample. Error bars show the standard deviation of over 1000 measured particle diameters for each size distribution. Inset: representative transmission electron micrograph of Pt-nanoparticles when 0.0015 wt % PVP is used in the synthesis.

The ratio of nanoparticle number to polymeric chain number in the samples prepared here utilizes 2−4 orders of magnitude less polymer than typically reported in the literature[15,19,20] (see the Supporting Information for Pt-nanoparticle concentration calculation). For our work, the presence of excess PVP in the continuous phase is ultimately detrimental as its ability to physisorb to a broad range of interfaces[16] means that free polymer and nanoparticles will compete for adsorption sites on the surfaces of interest. We therefore studied the influence of the polymer concentration used in the nanoparticle synthesis (and the resulting likely excess of polymer chains in the continuous phase) on the resulting Pt-nanoparticle adsorption density using both QCM and TEM.

Initial PVP Stabilizer Concentration and Its Effect on Pt-Nanoparticle Adsorption Density. QCM was used to explore Pt-nanoparticle adsorption densities on spin coated pEMA films, as a function of the PVP concentration used in the Pt-nanoparticle synthesis. The same set of nanoparticle dispersions were also adsorbed onto pEMA coated TEM grids by dipping these grids into the dispersions for 30 min (chosen to ensure adsorption equilibrium), before washing with copious amounts of Milli-Q water. Figure 2 compares the data acquired by both techniques. Figure 2a−d shows TEM images of the adsorbed Pt-nanoparticles on the pEMA-coated grids, and Figure 2e (squares) shows the measured Pt-nanoparticle density converted to mass per unit area (using image-j and the previously calculated mean particle diameter) as a function of PVP concentration. Figure 2e (circles) also shows the corresponding adsorbed mass obtained from QCM measurements using a pEMA-coated quartz crystal (converted using Sauerbrey's equation[17]) as a function of PVP concentration. The blue triangle represents the converted adsorbed mass measured via QCM for pure PVP, at a bulk concentration of 2 wt % which is equivalent to the highest concentration of PVP used to synthesize the Pt-nanoparticles.

DOI: 10.1021/acs.langmuir.7b02874
Langmuir 2018, 34, 1473−1480

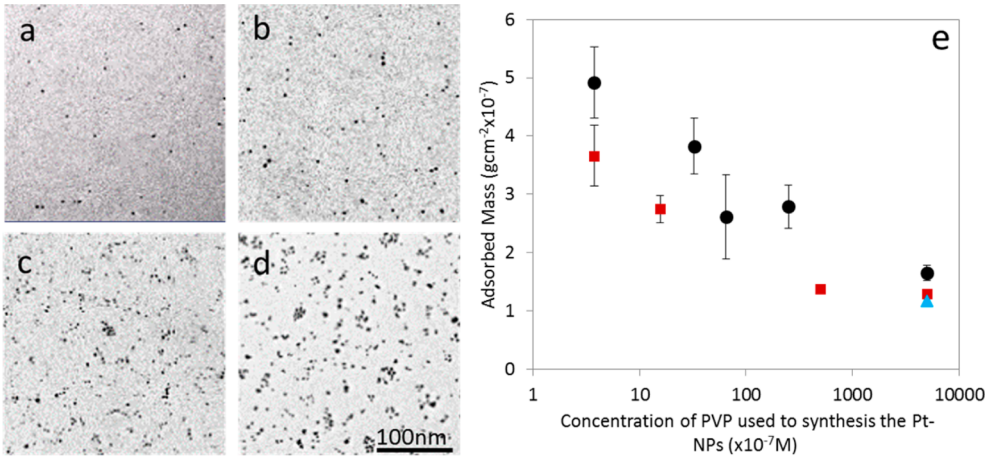

Figure 2. (a–d) Representative transmission electron micrographs of the resulting Pt-nanoparticle adsorbed onto the pEMA-coated grid. Adsorption densities can be seen to increase as a function of decreasing concentration of PVP used to synthesize the Pt-nanoparticles (a) 2 wt %, (b) 0.2 wt %, (c) 0.065 wt %, and (d) 0.0015 wt %. (e, squares) Measured Pt-nanoparticles adsorption density as mass per unit surface area measured by TEM as a function of PVP concentration. (e, circles) QCM mass adsorption data as a function of PVP concentration. Blue triangle represents the adsorbed mass recorded via QCM for pure PVP at 2 wt %.

Reducing the concentration of PVP stabilizer used in the original nanoparticle synthesis results in a visible increase in Pt-nanoparticle adsorption density, and consequently an increase in the measured adsorbed mass derived from both the QCM data (Figure 2e) and TEM data (Figure 2a–d and e, squares). For the highest polymer concentration used in the synthesis, the adsorbed mass recorded with both the QCM and the TEM becomes similar to the adsorbed mass of pure polymer in the bulk at the same concentration, suggesting that very few Pt-nanoparticles can be adsorbed under these conditions. The lack of contrast between the underlying carbon grid and the PVP chains means that calculations of mass per unit area based on the TEM images do not take account of the adsorbed free PVP or the PVP stabilizer around each nanoparticle core. We accounted for the adsorbed polymer mass on the surface by adding the value for adsorbed mass measured via QCM for pure PVP at the corresponding concentration to the TEM adsorbed mass data for all samples.

As the polymer concentration used in the original nanoparticle synthesis is increased, free polymer competes with the nanoparticles for adsorption sites on the pEMA-coated substrates and both restrict further adsorption of either species by steric hindrance. Figure 2a–d shows pEMA films saturated with a combination of free PVP and PVP stabilized Pt-nanoparticles. It is worth noting here that for both the QCM and TEM experiments, the Pt-nanoparticles are in excess in the bulk suspension as compared to the available total surface area.

It is worth noting that there are no chemical differences between the excess polymer and the nanoparticle surface and size/molecular weight differences are not large enough to allow for separation of the free PVP and PVP-coated NPs. As a result, a suitable concentration of PVP (0.0015 wt %) in the nanoparticle synthesis that limits excess PVP while maintaining nanoparticle stability, and maximizes Pt-nanoparticle adsorption density, was identified. In all subsequent experiments, this particular concentration of PVP will be used for the nanoparticle synthesis.

Next, the effect of dilution on the Pt-nanoparticle adsorption is explored to maximize the efficiency of the adsorption process onto capsule surfaces. This is important to ensure reproducibility of the adsorption process for different concentrations of microcapsules to be coated in the final application. However, dilution of the particle suspension for the adsorption process will affect the kinetics of adsorption, which we also investigate here via QCM and TEM. The Langmuir adsorption model is typically used extensively in the literature to understand the adsorption of small molecules onto surfaces. However, it has also been used to model the adsorption process of more complex systems such as polymer stabilized nanoparticles.[21−24] In our case, we measure the kinetics of adsorption with a QCM and apply this model to the resultant data to attempt to gain further insight.

Langmuir Adsorption Model. Adsorption data as a function of time over a range of Pt-nanoparticle suspension concentrations, shown in Figure 3, were used to analyze both the kinetics and the equilibrium condition using Langmuir adsorption theories. Analysis of these data allows us to determine a consistent value of the Langmuir adsorption equilibrium constant for the Pt-nanoparticle–substrate surface (pEMA) interaction.[22]

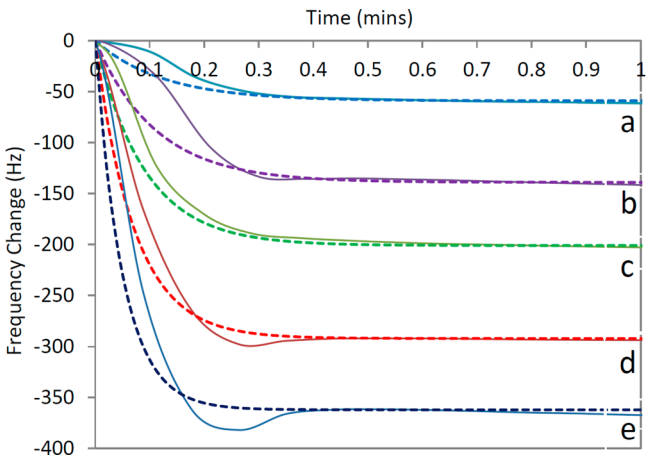

Figure 3. Recorded data from QCM adsorption experiments for different concentrations of Pt-nanoparticles at concentrations of (a) 2.8×10^{14}, (b) 5.5×10^{14}, (c) 1.2×10^{15}, (d) 2.3×10^{15}, and (e) 4.6×10^{15} Pt-nanoparticles mL^{-1}. Respective fits for each isotherm are represented by the dotted lines (eq 2).

DOI: 10.1021/acs.langmuir.7b02874
Langmuir 2018, 34, 1473−1480

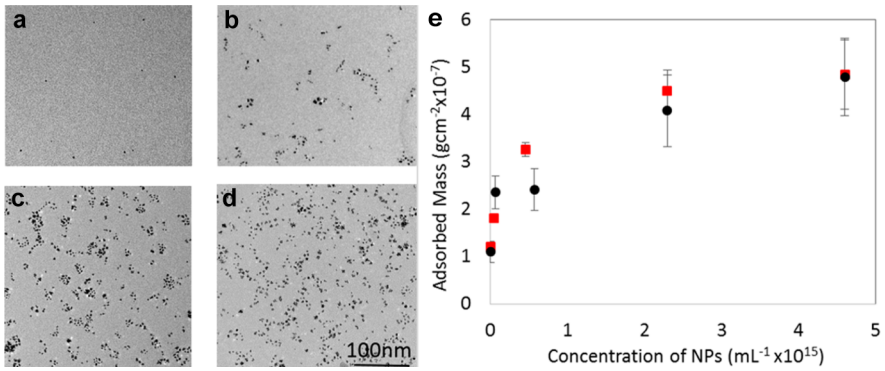

Figure 4. (a–d) TEM micrographs of the resulting Pt-nanoparticle adsorption density when different dilutions of Pt-nanoparticles (original Pt-nanoparticles dispersion synthesized using 0.0015 wt % PVP (a) 100%, (b) 50%, (c) 10%, and (d) 1% of the original suspension concentration respectively) are introduced to pEMA films on dip coated TEM grids. (e, squares) Corresponding measured Pt-nanoparticle density, converted to mass per unit area, as a function Pt-nanoparticle dilution. (e, circles) Resulting mass adsorption, calculated from the QCM frequency change, that occurs when the same series of Pt-nanoparticle suspension dilutions are introduced to a 2D model pEMA spin coated crystal.

The adsorption kinetics are quantified by fitting the measured QCM adsorption data (Figure 3) using eq 2. The Sauerbrey approach shows that the change in frequency (Δf) is proportional to the adsorbed mass and therefore to the adsorbed surface density. Therefore, Δf at equilibrium and Δf at time (t) can be used as proxies for $\Gamma(\infty)$ and $\Gamma(t)$, respectively, in eq 2. Values of the rate constant k_0 can then be estimated by fitting the data collected from the QCM. From eq 3, plotting k_0 as a function of nanoparticle concentration (C), the intercept and gradient correspond to the desorption (k_d) and adsorption (k_a) constants, respectively. The Langmuir equilibrium constant (K_L) is then defined as (k_a/k_d) and is a measure of the depletion per unit volume of the surface active species from the bulk.

$$\Gamma(t) = \Gamma(\infty)[1 - \exp(-k_0 t)] \tag{2}$$

$$k_0 = k_a C + k_d \tag{3}$$

$$\Gamma(\infty) = C/(C + k_d/k_a) \tag{4}$$

where Γ is nanoparticle surface coverage (ΔHz), C is nanoparticle concentration (mol/L), k_a is adsorption rate constant ((mol/L)$^{-1}$s^{-1}), k_d is desorption rate constant (s^{-1}), and t is time (s).

To conform to previous attempts in the literature to quantify the concentration of Pt-nanoparticles in a manner suitable for running the Langmuir adsorption model, the concentration was calculated in moles per liter. The number of nanoparticles per liter was first calculated and subsequently divided by Avogadro's number to convert to an equivalent "moles per liter" value (see the Supporting Information for details). The dispersion concentration was found to be 7.7 μmol L^{-1} prior to dilution.

Figure 3 shows the observed QCM data for different Pt-nanoparticle suspension concentrations. The respective fits for each isotherm are represented by the dotted lines (eq 2).

Δf absolute values increase with increasing Pt-nanoparticle suspension concentration, and all graphs are seen to plateau in less than 30 s (Figure 3). Note that the overshoot in frequency change is due to the hydrodynamic forces caused by the valve opening on the QCM inflow as previously observed by other authors.[25]

The Langmuir model provides a way of calculating adsorption and desorption constants for interfacial-active species. Of course, as mentioned above, it is clear that the nanoparticles in our system do not effectively desorb from the substrate, which potentially reduces the usefulness of the Langmuir model. This is a well-known challenge for high molecular weight polymers or other species (such as nanoparticles) that do not desorb from the substrate in the experimental time frame. Indeed, despite the good fit to our data, the model in this case drastically underpredicts the desorption energy (approximately a few kT from the fit to the QCM data (see the Supporting Information for calculations)).

In addition, we observe large differences in final (at equilibrium) adsorbed masses recorded by the QCM as the suspension is diluted. A likely explanation for this is as follows. If only one species was present with a very low desorption rate, one would expect the final adsorption density (independently of adsorption rate) to be the same at all concentrations in the presence of an excess of the adsorbing species. The changes with dilution are indicative of the presence of a second competitive species, i.e. free polymer, with a different diffusion rate and adsorption energy. This is further confirmed when taking into account the time taken to reach equilibrium, which is almost constant independently of dilution ratios. As a result, this indicates that a faster diffusing species (i.e., the free PVP) appears to be compensating for the expected drop in adsorption rate as a result of lowered concentrations. It is very likely that this phenomenon will also influence the adsorption process of other similar polymer-stabilized nanoparticle systems, particularly when a high initial concentration of polymer stabilizer is used in the nanoparticle synthesis with resultant free polymer in solution. Thus, care should always be taken when concluding from modeling the adsorption process for these types of nanoparticles using the Langmuir adsorption model that additional effects due to the presence of secondary species are not missed. It is also clear that the Langmuir adsorption model is not appropriate for these strongly adsorbing complex systems.

Probing Further the Effect of Suspension Concentration on Pt-Nanoparticle Adsorption Density on 2D Model pEMA Films Using TEM. As previously explained, typical nanoparticle syntheses found in the literature routinely use a large excess of polymer stabilizer.[7,19,20] Typically the excess polymer is not removed from the bulk before the suspension is used. The free polymer will therefore affect the subsequent adsorption of the nanoparticles onto target

DOI: 10.1021/acs.langmuir.7b02874
Langmuir 2018, 34, 1473–1480

substrates. As our nanoparticle samples do contain a small excess of PVP in the suspension (even at the lowest concentration of PVP stabilizer tested here (0.0015 wt %)), we expect a competition between the free PVP and Pt-nanoparticles for adsorption on the polymer surface. If one species diffuses more rapidly, as we may expect, then this species should dominate the adsorption process, particularly at low concentrations. Here we test this question by estimating the ratio of free PVP to Pt-nanoparticles adsorbed at the interface using TEM.

A series of Pt-nanoparticle suspension dilutions (with Milli-Q water) were adsorbed to pEMA films on dip coated TEM grids and spin-coated pEMA films on QCM crystals. Figure 4a–d shows the resulting TEM micrographs of the adsorbed Pt-nanoparticles, and Figure 4e (squares) gives the corresponding adsorbed mass data. For comparison, the QCM adsorption data are also shown in Figure 4e (circles), calculated using the Sauerbrey equation.

The adsorbed mass per unit area is seen to increase with increasing nanoparticle suspension concentration (Figure 4). These results provide further evidence that free PVP will block potential nanoparticle adsorption sites and, at a constant ratio of Pt-nanoparticles to free PVP in the bulk, the Pt-nanoparticles can more effectively compete for surface adsorption sites at higher concentrations. It is worth noting here that some excess salt will be present in the original suspension as a consequence of our synthesis method. Therefore, as this suspension is diluted with Milli-Q water to vary the particle concentration, the electrolyte concentration will also be reduced which will have some effect on the frequency change observed in the QCM. However, the expected frequency change for salt present in our most concentrated Pt-nanoparticle suspension relative to pure water can be calculated to be approximately 5% of the total frequency change observed.[26] In addition, Jhon et al.[27] show similar small changes experimentally. The TEM data also agree well with the data from the QCM. Indeed, Figure 2E demonstrates that adsorption of PVP alone in solution in water gives an adsorbed mass comparable to a nanoparticle suspension with a high excess of polymer in the continuous phase when electrolyte is present as a result of the particle synthesis.

An explanation for the observed trend could be that as the suspension is diluted, the average distance to reach the interface for each species increases. A particles displacement is proportional to the diffusion coefficient.[28] Therefore, if the diffusion coefficient of the PVP is larger than the Pt-nanoparticles, as superficially expected, then the PVP will increasingly beat the Pt-nanoparticles to the interface as the concentration is reduced.

The Pt-nanoparticles consist of a platinum core surrounded by polymer, as demonstrated by the stability of the dispersions and the adsorbed nanoparticle spacing observed on the TEM micrographs. It can be argued therefore that the Pt-nanoparticles behave more like larger polymer entities rather than hard particles.

Georges uses eq 5 to calculate diffusion coefficients for polymers in an aqueous environment.[29] For an ideal chain, eq 6 can then be used to calculate a radius of gyration for the same polymer (see the Supporting Information for PVP radius of gyration calculation).[30] If this radius is then used in the Stokes–Einstein (eq 7), usually used to calculate diffusion coefficients for hard spherical particles, one obtains diffusion coefficient values which are consistent with those calculated from eq 5.

$$D = 1.25(10^{-4})M_w^{-0.55} \tag{5}$$

$$R_g \approx bN^{1/2} \tag{6}$$

$$D = \frac{k_B T}{6\pi\eta r} \tag{7}$$

where D is the diffusion coefficient ($m^2\ s^{-1}$), k_B is the Boltzmann constant $1.38 \times 10^{-23}\ m^2\ kg\ s^{-2}\ K^{-1}$ ($1.38 \times 10^{-20}\ m^2\ g\ s^{-2}\ K^{-1}$), η is the dynamic viscosity 1×10^{-3} Kg s^{-1} m^{-1} (1.0 g s^{-1} m^{-1}), r is the radius of the spherical particle (m), T is temperature (K), R_g is radius of gyration (m), N is the number of monomers, b is intermonomer spacing, and M_w is molecular weight (g mol^{-1}) (PVP used here 40 000 g·mol^{-1}).

At the low PVP concentrations used in this study, the ratio of introduced PVP chains to synthesized Pt-nanoparticles can be shown to be approximately 1:1, nanoparticles would appear to consist of a platinum core embedded within single PVP polymeric chains. The difference in diameter between a free PVP chain and the Pt-nanoparticle was found by comparing the radius of gyration of 40 KDa PVP to the radius from a sphere created from the combined volume of the Pt core and PVP chains volume of gyration (an assumption was made that the PVP chain volume changed little on association with the Pt core). On this basis values for the diffusion coefficients of the free PVP and Pt-nanoparticle were found to be 3.68×10^{-11} and $3.19 \times 10^{-11}\ m^2\ s^{-1}$, respectively.

This difference between the diffusion rates of free polymer and the nanoparticles and its potential effect on nanoparticle adsorption density is likely to be an inherent issue when attempting to adsorb nanoparticle suspensions which are stabilized by polymeric species which are themselves surface active. As previously described, in the literature, authors typically use a large excess of polymer as stabilizer[15,19,20] and little work has been done to significantly reduce this excess without compromising stability.

In this study, the nanoparticles only need to remain stable for a short amount of time (typically <1 day) before they are used for adsorption onto the relevant surfaces. Over this period of time, and indeed up to 6 weeks, there is no evidence of particle destabilization.

Pt-Nanoparticle Adsorption on 3-D Microcapsule Interfaces. An equivalent adsorption experiment was conducted on the surface of a preprepared toluene core pEMA shell microcapsule sample in order to test the effects of moving from a 2-D to 3-D substrate. Pt-nanoparticles suspensions at different concentrations were added to microcapsule dispersions at a constant concentration. TEM images were analyzed manually and the measured Pt-nanoparticle surface densities were corrected for curvature and capsule transparency (see the Supporting Information).

Figure 5 (diamonds) shows a graph of Pt-nanoparticle adsorption densities on the 3D polymeric microcapsule surfaces as a function of Pt-nanoparticle concentration. The equivalent adsorption data for 2D model substrates analyzed using TEM is also plotted (Figure 5 squares). The inset shows a TEM micrograph of a single capsule which has undergone Pt-nanoparticle adsorption.

Even though there has been a dramatic increase in available surface area of ~20 000 times (see the Supporting Information

DOI: 10.1021/acs.langmuir.7b02874
Langmuir 2018, 34, 1473–1480

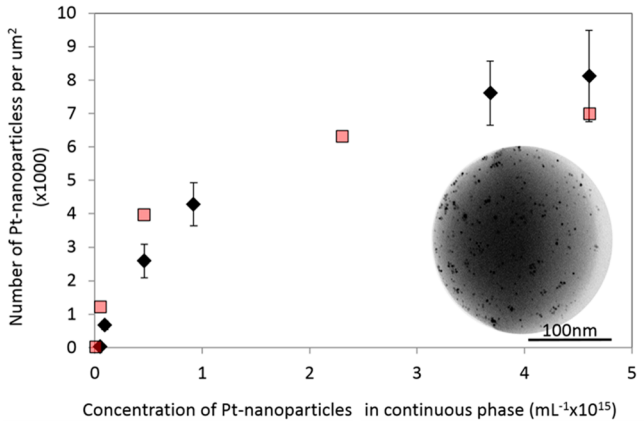

Figure 5. Graph showing Pt-nanoparticle adsorption density on the 3D polymeric microcapsule surfaces as a function of concentration of the Pt-nanoparticle suspension (diamonds). Equivalent adsorption data for 2D model substrates analyzed using TEM is also shown (squares). Inset shows a TEM micrograph of a single capsule which has undergone Pt-nanoparticle adsorption.

for colloidal dispersion surface area calculation), the resulting Pt-nanoparticle density at saturation is approximately the same for the 2-D model system and the 3-D capsules. One of our aims is to have control over the Pt-nanoparticle density independent of concentration of microcapsules introduced, Pt-nanoparticle adsorption density at equilibrium being independent of surface area introduced achieves this.

In order to show that these results were not caused by depletion of Pt-nanoparticles from the bulk the number of Pt-nanoparticles available in the bulk per unit surface area of capsules introduced for each dispersion concentration was compared to the measured Pt-nanoparticle adsorption densities on the polymeric microcapsule surface and was shown to be significantly greater, in all cases.

Figure 6[1] shows representative TEM images of the Pt-nanoparticle loaded capsules. Insets to (a) and (d) show the

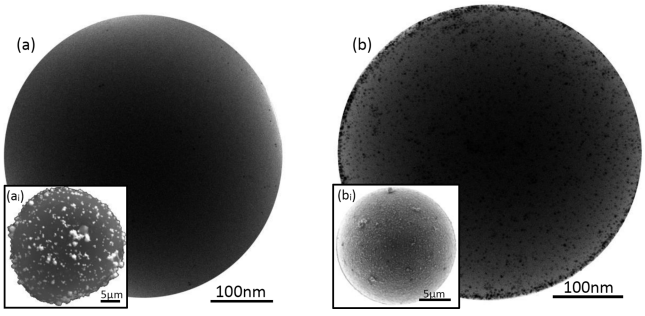

Figure 6. (a,b) Representative TEM micrographs of the poor and good Pt-nanoparticle loaded microcapsules. Insets (a_i)[1] and (b_i) show the corresponding poor and good gold coated capsules as a result of the different densities of adsorbed Pt-nanoparticles.

corresponding poor and good gold coated capsules on capsules with different densities of adsorbed Pt-nanoparticles. This provides a graphic example of why having good control over the Pt-nanoparticle surface density is important for growing metal films on catalytic nanoparticle films via electroless deposition.

CONCLUSION

We have studied the adsorption of sterically stabilized metallic nanoparticles onto polymeric substrates, which is an important process used to physically immobilize catalytic nanoparticles on surfaces. As a result, our study is not only important for the subsequent electroless deposition processes we are aiming for in permanently encapsulating small molecules, but also relevant in other areas such as the drive for enhanced recovery of heterogeneous catalysts. Here, we considered the adsorption of PVP stabilized Pt-nanoparticles using QCM and TEM on model 2D spin-coated films and dip-coated TEM grids, respectively. Both the adsorption kinetics and resulting nanoparticle densities are characterized through this process. As a result, we demonstrate that excess polymer, which is often used in nanoparticle synthesis and subsequently overlooked in the literature, can compete with and thus drastically affect the adsorption of the Pt-nanoparticles. This limitation in the particle adsorption onto polymeric surfaces is subsequently used to optimize the adsorbed nanoparticle densities onto polymeric microcapsules to achieve a more efficient secondary metal growth. We expect this understanding can also be applied when these types of particles are used for their catalytic properties in other applications.

ASSOCIATED CONTENT

Supporting Information

The Supporting Information is available free of charge on the ACS Publications website at DOI: 10.1021/acs.langmuir.7b02874.

Langmuir adsorption modeling, calculation of colloidal surface areas and dispersion concentration, calculation of ratios of PVP to Pt-nanoparticles used in our system, measurement of Pt-nanoparticle surface density on 3D capsules using TEM, QCM crystal multiple wash cycles (PDF)

AUTHOR INFORMATION

Corresponding Author

*E-mail: J.P.Hitchcock@leeds.ac.uk.

ORCID

James P. Hitchcock: 0000-0003-2226-6734

Notes

The authors declare no competing financial interest.

ACKNOWLEDGMENTS

The authors gratefully acknowledge the Engineering and Physical Sciences Research Council (EP/H501355/1, EP/J500458/1, EP/K503836/1) and Procter and Gamble for their generous support of this work.

REFERENCES

(1) Hitchcock, J. P.; Tasker, A. L.; Baxter, E. A.; Biggs, S.; Cayre, O. J. Long-Term Retention of Small, Volatile Molecular Species within Metallic Microcapsules. *ACS Appl. Mater. Interfaces* **2015**, *7*, 14808−14815.

(2) Álvarez-Paino, M.; Marcelo, G.; Muñoz-Bonilla, A.; Fernández-García, M. Catecholic chemistry to obtain recyclable and reusable hybrid polymeric particles as catalytic systems. *Macromolecules* **2013**, *46*, 2951−2962.

(3) del Mercato, L. L.; Gonzalez, E.; Abbasi, A. Z.; Parak, W. J.; Puntes, V. Synthesis and evaluation of gold nanoparticle-modified

DOI: 10.1021/acs.langmuir.7b02874
Langmuir 2018, 34, 1473−1480

polyelectrolyte capsules under microwave irradiation for remotely controlled release for cargo. *J. Mater. Chem.* **2011**, *21*, 11468−11471.
(4) Bédard, M. F.; De Geest, B. G.; Skirtach, A. G.; Möhwald, H.; Sukhorukov, G. B. Polymeric microcapsules with light responsive properties for encapsulation and release. *Adv. Colloid Interface Sci.* **2010**, *158*, 2−14.
(5) Cayre, O. J.; Biggs, S. Hollow microspheres with binary porous membranes from solid-stabilised emulsion templates. *J. Mater. Chem.* **2009**, *19*, 2724−2728.
(6) Yun, G.; Hassan, Z.; Lee, J.; Kim, J.; Lee, N. S.; Kim, N. H.; Baek, K.; Hwang, I.; Park, C. G.; Kim, K. Highly Stable, Water-Dispersible Metal-Nanoparticle-Decorated Polymer Nanocapsules and Their Catalytic Applications. *Angew. Chem., Int. Ed.* **2014**, *53*, 6414−6418.
(7) Antipov, A. A.; Sukhorukov, G. B.; Fedutik, Y. A.; Hartmann, J.; Giersig, M.; Möhwald, H. Fabrication of a novel type of metallized colloids and hollow capsules. *Langmuir* **2002**, *18*, 6687−6693.
(8) Liu, D.; Jiang, X.; Yin, J. One-Step Interfacial Thiol−Ene Photopolymerization for Metal Nanoparticle-Decorated Microcapsules (MNP@ MCs). *Langmuir* **2014**, *30*, 7213−7220.
(9) Anandhakumar, S.; Vijayalakshmi, S.; Jagadeesh, G.; Raichur, A. M. Silver nanoparticle synthesis: novel route for laser triggering of polyelectrolyte capsules. *ACS Appl. Mater. Interfaces* **2011**, *3*, 3419−3424.
(10) Kozlovskaya, V.; Kharlampieva, E.; Chang, S.; Muhlbauer, R.; Tsukruk, V. V. pH-Responsive Layered Hydrogel Microcapsules as Gold Nanoreactors. *Chem. Mater.* **2009**, *21*, 2158−2167.
(11) De Geest, B. G.; Skirtach, A. G.; De Beer, T. R.; Sukhorukov, G. B.; Bracke, L.; Baeyens, W. R.; Demeester, J.; De Smedt, S. C. Stimuli-Responsive Multilayered Hybrid Nanoparticle/Polyelectrolyte Capsules. *Macromol. Rapid Commun.* **2007**, *28*, 88−95.
(12) Caruso, F.; Spasova, M.; Salgueiriño-Maceira, V.; Liz-Marzán, L. Multilayer Assemblies of Silica-Encapsulated Gold Nanoparticles on Decomposable Colloid Templates. *Adv. Mater.* **2001**, *13*, 1090−1094.
(13) Skirtach, A. G.; Dejugnat, C.; Braun, D.; Susha, A. S.; Rogach, A. L.; Parak, W. J.; Möhwald, H.; Sukhorukov, G. B. The role of metal nanoparticles in remote release of encapsulated materials. *Nano Lett.* **2005**, *5*, 1371−1377.
(14) Liu, D.; Jiang, X.; Yin, J. One-Step Interfacial Thiol−Ene Photopolymerization for Metal Nanoparticle-Decorated Microcapsules (MNP@MCs). *Langmuir* **2014**, *30*, 7213−7220.
(15) Horiuchi, S.; Nakao, Y. Platinum colloid catalyzed etchingless gold electroless plating with strong adhesion to polymers. *Surf. Coat. Technol.* **2010**, *204*, 3811−3817.
(16) Haaf, F.; Sanner, A.; Straub, F. Polymers of N-vinylpyrrolidone: synthesis, characterization and uses. *Polym. J.* **1985**, *17*, 143−152.
(17) Sauerbrey, G. Verwendung von Schwingquarzen zur Wägung dünner Schichten und zur Mikrowägung. *Eur. Phys. J. A* **1959**, *155*, 206−222.
(18) Kamyshny, A.; Magdassi, S. Aqueous dispersion of metallic nanoparticles. *Nanoscience colloidal and interfacial*, 1st ed.; CRC Press: New York, 2009; pp 747−778.
(19) Pastoriza-Santos, I.; Liz-Marzán, L. M. Formation of PVP-Protected Metal Nanoparticles in DMF. *Langmuir* **2002**, *18*, 2888−2894.
(20) Jiang, S. P.; Li, L.; Liu, Z.; Pan, M.; Tang, H. L. Self-Assembly of PDDA-Pt Nanoparticle/Nafion Membranes for Direct Methanol Fuel Cells. *Electrochem. Solid-State Lett.* **2005**, *8*, A574−A576.
(21) Groenzin, H.; Mullins, O. C. Molecular size and structure of asphaltenes from various sources. *Energy Fuels* **2000**, *14*, 677−684.
(22) Park, J. J.; Lacerda, S. H. D. P.; Stanley, S. K.; Vogel, B. M.; Kim, S.; Douglas, J. F.; Raghavan, D.; Karim, A. Langmuir adsorption study of the interaction of CdSe/ZnS quantum dots with model substrates: influence of substrate surface chemistry and pH. *Langmuir* **2009**, *25*, 443−450.
(23) Rudrake, A.; Karan, K.; Horton, J. H. A combined QCM and XPS investigation of asphaltene adsorption on metal surfaces. *J. Colloid Interface Sci.* **2009**, *332*, 22−31.
(24) Ekholm, P.; Blomberg, E.; Claesson, P.; Auflem, I. H.; Sjöblom, J.; Kornfeldt, A. A quartz crystal microbalance study of the adsorption of asphaltenes and resins onto a hydrophilic surface. *J. Colloid Interface Sci.* **2002**, *247*, 342−350.
(25) Xu, D.; Hodges, C.; Ding, Y.; Biggs, S.; Brooker, A.; York, D. A QCM study on the adsorption of colloidal laponite at the solid/liquid interface. *Langmuir* **2010**, *26*, 8366−8372.
(26) Kanazawa, K. K.; Gordon, J. G. Frequency of a quartz microbalance in contact with liquid. *Anal. Chem.* **1985**, *57*, 1770−1771.
(27) Jhon, Y. K.; Bhat, R. R.; Jeong, C.; Rojas, O. J.; Szleifer, I.; Genzer, J. Salt-Induced Depression of Lower Critical Solution Temperature in a Surface-Grafted Neutral Thermoresponsive Polymer. *Macromol. Rapid Commun.* **2006**, *27*, 697−701.
(28) Seisenberger, G.; Ried, M. U.; Endress, T.; Büning, H.; Hallek, M.; Bräuchle, C. Real-time single-molecule imaging of the infection pathway of an adeno-associated virus. *Science* **2001**, *294*, 1929−1932.
(29) Georges, J. Investigation of the diffusion coefficient of polymers and micelles in aqueous solutions using the Soret effect in cw-laser thermal lens spectrometry. *Spectrochim. Acta, Part A* **2003**, *59*, 519−524.
(30) Flory, P. J.; Volkenstein, M. Statistical mechanics of chain molecules. *Biopolymers* **1969**, *8*, 699−700.

DOI: 10.1021/acs.langmuir.7b02874
Langmuir 2018, 34, 1473−1480